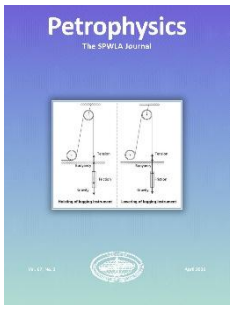

Petrophysics Vol. 67 No. 2 April 2026

TABLE OF CONTENTS PAGE

A Knowledge-Guided Data-Driven Method for Predicting Reservoir Parameters
Hongda Yu, Baozhi Pan, Yuhang Guo, Yixuan Wang, Yixuan Zhou, and Yan Li
PETROPHYSICS, VOL. 67, NO. 2 (APRIL 2026); PAGES 351–373; 14 FIGURES, 18 TABLES.
DOI:10.30632/PJV67N2-2026a7

Improving Fracture Complexity of Deep Shale Based on Induced Stress Difference: A Case Study of the Qiongzhusi Shale
Jianfa Ci
PETROPHYSICS, VOL. 67, NO. 2 (APRIL 2026); PAGES 374–385; 9 FIGURES, 2 TABLES.
DOI:10.30632/PJV67N2-2026a8

Acid Fracturing-Induced Fracture Propagation in Deep Coalbed Methane Wells: A Case Study in Daning-Jixian Block
Haifeng Zhao, Bingquan Jin, Huabin Zhen, and Shuguang Li
PETROPHYSICS, VOL. 67, NO. 2 (APRIL 2026); PAGES 386–403; 13 FIGURES, 6 TABLES.
DOI:10.30632/PJV67N2-2026a9

Analysis of the Dynamic Interlayer Fracture Propagation Behavior of Hydraulic Fractures in Interbedded Coal-Bearing Strata—A Case of the Taiyuan Formation in the Jiyang Depression
Zhihong Zhao, Haozeng Jin, Jianchun Guo, Shiqian Xu, Kaiwen Xue, and Zilin Zhang
PETROPHYSICS, VOL. 67, NO. 2 (APRIL 2026); PAGES 404–419; 13 FIGURES, 6 TABLES.
DOI:10.30632/PJV67N2-2026a10

Cementing

New Equipment and Method for Evaluating Anti-Water-Invasion Ability of Cement Slurry
Xiayu Zhang, Xingguo Zhang, Tuoming Zhang, Xiangyin Li, Chao Mei, Bo Li, Ming Jiang, Kaiqiang Liu, and Yang Ba
PETROPHYSICS, VOL. 67, NO. 2 (APRIL 2026); PAGES 421–435; 11 FIGURES, 2 TABLES.
DOI:10.30632/PJV67N2-2026a11

Technical Briefing

Automatic Well-Log Depth Shifting With Data-Driven Approaches: A Contest Summary
Wen Pan, Lei Fu, Chicheng Xu, Michael Ashby, Hyungjoo Lee, Jaehyuk Lee, Fan Meng, Siyuan Chen, Yingying Ye, Hailong Jiang, Hyunmin Kim, Heesung Kong, Inwook Baek, Jinhyeon Baek, Xuekai Sun4, Hao Sun4, Siyi Li4, ZiMeng Zhao4, Yuxin Ke5, Chuang Hei5, Ankang Feng5, Wei Hu5, Yifan Wu, Byunghoon Choi, Hojin Kang, and JunHa Park
PETROPHYSICS, VOL. 67, NO. 2 (APRIL 2026); PAGES 437–462; 17 FIGURES, 3 TABLES.
DOI:10.30632/PJV67N2-2026a12

HOW TO ACCESS ARTICLES

SPWLA Members have access to journals through paid membership packages. Annual dues include digital issues of Petrophysics Journal. Sign into your account Visit tab Publications → Petrophysics Papers.
Expired Membership? Sign into your account https://www.spwla.org/SPWLA/Members/MemberHome.aspx to make payment. Reset maybe delayed by until the next SPWLA business day.
Become a member? Join now https://www.spwla.org/SPWLA/Membership/Join_Now/Become_a_Member.aspx?hkey=902c4b79-2640-4b86-a56b-609e20248ba6

APRIL 2026 PAPER SUMMARIES

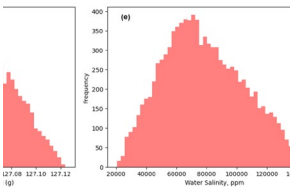

Alghazal and Krinis **PAGES 248–262**

This paper presents an uncertainty assessment of lab-derived fluid saturation data from sponge cores using deterministic sensitivity analysis and Monte Carlo simulation. The results identify water salinity as the primary factor influencing the calculated oil saturation and introduce analytical and iterative models to estimate salinity and refine saturation calculations, improving the reliability of core-based reservoir evaluation.

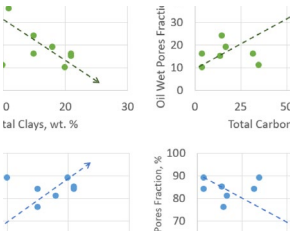

Aljishi et al. **PAGES 263–279**

This paper presents an NMR T_2-based workflow to quantify pore-type wettability partitioning across 12 unconventional core samples and relates it to mineralogy and dual-fluid displacement behavior. The results show that silica/clay-rich rocks are dominated by mixed-wet pores, while carbonate-rich rocks exhibit higher oil-wet fractions and a consistent brine preference under competitive displacement. An oil saturation choking threshold (26 to 71%) is also defined as a screening metric for evaluating the potential benefit of brine-based choking prior to flowback.

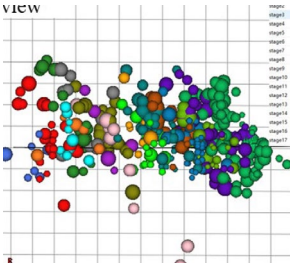

Ci **PAGES 374–385**

Regarding shale fracturing of the Qiongzhusi Formation in southern Sichuan, existing research has paid little attention to the effects of displacement and fluid volume on the stress field during single-stage fracturing, resulting in uncertainty in field design. This study uses a finite discrete element method, combined with ZY-1 well parameters, to establish a two-dimensional model. It analyzes the influence of displacement and inflow on the stress field, clarifies the characteristics of the induced stress distribution, and optimizes construction parameters. Field application shows a significant improvement in fracture complexity.

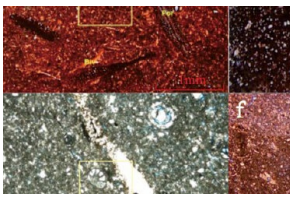

Guo et al. **PAGES 336–350**

Based on the hydrodynamic conditions in depositional environments, grain types in the Mishrif Formation were categorized into high-energy, moderate-energy, and low-energy grains. Through parameter clustering analysis, 16 lithofacies types were consolidated into seven geological facies based on the proportional relationships among low-energy grains, high-energy grains, and micritic matrix. The presence of high-energy grains promotes the formation of high-quality reservoirs.

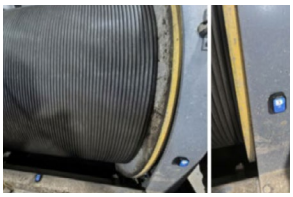

Liu et al. **PAGES 295–317**

During downhole operations in complex geological formations, wireline logging instruments are susceptible to operational anomalies, including downhole obstructions and jamming. Therefore, this paper proposes a dual-signal fusion analysis method for anomaly diagnosis based on cable tension and winch vibration. Both laboratory and on-site experiments show that this method can accurately identify downhole instrument anomalies, effectively reducing missed and false alarms.

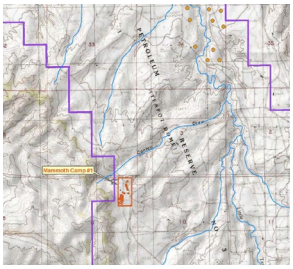

Pan et al. **PAGES 437–462**

This paper presents the results of the 2023 SPWLA PDDA Machine-Learning Competition, the first public benchmark comparing automated well-log depth-shifting methods. Using the Teapot Dome data set, the study evaluates a range of machine-learning and dynamic time warping (DTW)-based workflows, including deep learning, classical models, and algorithmic approaches, and shows that hybrid prediction-plus-DTW methods achieve the most accurate depth alignment. These findings highlight the promise of data-driven depth-shifting workflows in reducing manual preprocessing efforts and improving consistency in petrophysical interpretation.

APRIL 2026 PAPER SUMMARIES

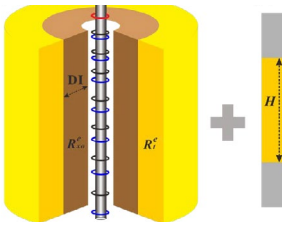

Qiao et al. **PAGES 318–334**

This paper presents a new hierarchical correction data processing method to accurately and rapidly obtain the true resistivity of tight sandstone reservoirs in horizontal wells. The proposed method simplifies the complex 3D inversion problem through model decomposition and correction coefficient construction, thereby achieving high-efficiency and high-precision inversion performance, as verified by field cases. This provides a reliable approach for tight sandstone reservoir evaluation.

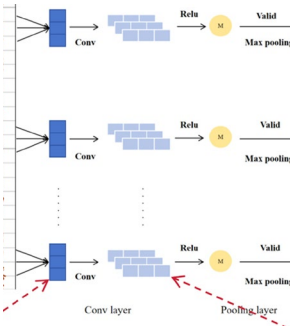

Yu et al. **PAGES 351–373**

This paper focuses on the Sulige area of the Ordos Basin, integrating a data-driven approach with petrophysical models to achieve high-precision predictions of key reservoir parameters, including porosity, water saturation, and permeability. A DCDNN model was constructed and optimized using the MPDG algorithm and Bayesian optimization, which significantly improved the representational capacity and predictive performance of the model. Finally, an expert committee-based decision-making mechanism was established using an ensemble learning theory. The selected optimal integrated model substantially reduced prediction errors and achieved excellent performance in blind well applications, providing reliable technical support for regional geological structure analysis and resource assessment.

Zhang et al. **PAGES 421–435**

This study proposes a novel method to rapidly evaluate the anti-water invasion (AWI) performance of cement slurries and assess water invasion during coagulation. The experimental results demonstrate that AWI materials enhance cement particle cohesion, effectively delaying water invasion and reducing ion loss in low-permeability cores compared with conventional slurries in high-permeability cores. This approach provides a foundation for optimizing AWI cement systems to improve cementing quality in adjustment wells.

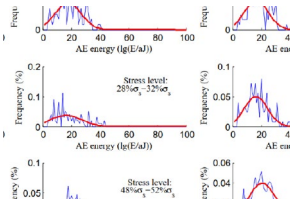

Zhao **PAGES 280–293**

This study conducted uniaxial compression acoustic emission experiments on sandstone under various water conditions. It analyzed the variation in mechanical parameters and acoustic emission propagation attenuation coefficients with the soaking duration. Additionally, the energy release characteristics of acoustic emission were discussed based on the accelerated release theory and normal distribution theory.

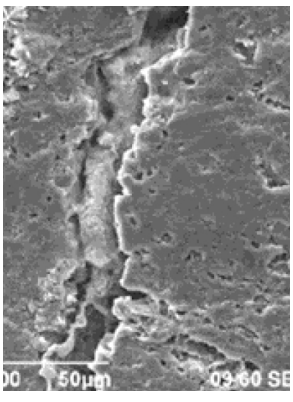

Zhao et al. **PAGES 386–403**

This study investigated acid-fracturing-induced fracture propagation in the deep No. 8 coal seam of the Daning-Jixian Block via triaxial hydraulic fracturing physical simulations and field tests, identifying 10% sulfamic acid as the optimal concentration and the coal seam roof as the preferred perforation location for forming complex fracture networks while controlling fracture height and ensuring construction safety. Perforating at the coal seam roof reduces the fracture initiation pressure and activates naturally weak surfaces in the coal seam to promote fracture branching, whereas an excessively high acid concentration causes uncontrolled fracture height and severe near-wellbore coal dissolution. The field application of the optimized acid fracturing scheme in Well J1 achieved a stable daily gas production of 11,000 m³ by forming an acid-dissolution-support composite fracture system, providing critical technical guidance for deep coalbed methane reservoir development.

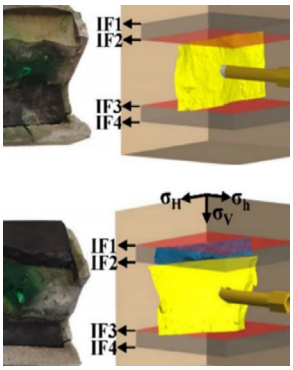

Zhao et al. **PAGES 404–419**

Aiming at the multilayered deposition of sand, coal, and mudstone with high hydrocarbon content in the Jiyang Depression, a finite discrete element model was established to analyze the effects of the fracturing layer, pumping rate, liquid viscosity, and cleat connectivity on the longitudinal propagation of hydraulic fractures in interbedded coal formations. The results indicate that sandstone as the fracturing layer enables hydraulic fractures to cross interlayer interfaces to transform coal seams, while coal rock as the fracturing layer confines fractures within the coal seam. The optimal fracturing parameters are recommended as 22 m^3/min pumping rate and 15 mPa·s liquid viscosity. Field practice shows that Well A in the Jiyang Depression achieves an average daily gas production exceeding 10,000 m^3/d and a maximum of over 20,000 m^3/d, with a significantly improved production effect.